Intracellular pH response to weak acid stress in individual vegetative Bacillus subtilis cells

Reference:

Pandey Rachna, Vischer Norbert O.E., Smelt Jan P.P.M., van Beilen Johan W.A., Ter Beek Alexander, De Vos Winnok, Brul Stanley, Manders Erik M.M..- Intracellular pH response to weak acid stress in individual vegetative Bacillus subtilis cells Applied and environmental microbiology - ISSN 0099-2240 - 82:21(2016), p. 1-11

Full text (Publishers DOI): http://dx.doi.org/doi:10.1128/AEM.02063-16

Intracellular pH response to weak acid stress in individual vegetative *Bacillus subtilis* cells

Rachna Pandey[1], Norbert O.E. Vischer[1], Jan P.P.M. Smelt[1], Johan W.A. van Beilen[1], Alexander Ter Beek[1], Winnok H. De Vos[2, 3*], Stanley Brul[1#*], Erik M.M. Manders[4*]

[1] Molecular Biology and Microbial Food Safety, SILS, University of Amsterdam, Amsterdam, The Netherlands.

[2] Department of Veterinary Sciences, Laboratory of Cell Biology and Histology, Antwerp University, Antwerpen, Belgium.

[3] Department Molecular Biotechnology, Cell Systems and Imaging Group, Ghent University, Ghent, Belgium.

[4] Van Leuwenhoek Centre for Advance Microscopy, SILS, University of Amsterdam, Amsterdam, The Netherlands.

Running title: Intracellular pH response to weak acid in single cells

[*]Contributed equally.

 # Corresponding author: Prof. dr. Stanley Brul

Mailing address: Molecular Biology and Microbial Food Safety, SILS, University of Amsterdam, Amsterdam, The Netherlands.

Phone: +31 205257079,

Fax: +31 205257934,

E-mail: s.brul@uva.nl

Keywords: *B. subtilis,* Intracellular pH, weak acid, single cell analysis, IpHluorin, Multichannel-SporeTracker

Abstract

The intracellular pH (pH_i) critically affects bacterial cell physiology. Hence, a variety of food preservation strategies aim at perturbing pH_i homeostasis. Unfortunately, accurate pH_i quantification with existing methods is suboptimal since measurements average across populations of cells, not taking into account inter-individual heterogeneity. Yet, physiological heterogeneity in isogenic populations is well known to be responsible for differences in growth and division kinetics of cells in response to external stressors. To assess in this context the behavior of intracellular acidity, we have developed a robust method to quantify pH_i at single-cell levels in *Bacillus subtilis*. Bacilli spoil food, cause disease and are well known for their ability to form highly stress-resistant spores. Using an improved version of the genetically encoded ratiometric pHluorin (IpHluorin), we have quantified pH_i in individual *B. subtilis* cells, cultured at an external pH of 6.4, in the absence or presence of weak acid stresses. In the presence of 3 mM potassium sorbate, a decrease in pH_i and an increase in the generation time of growing cells were observed. Similar, effects were observed when cells were stressed with 25 mM potassium acetate. Time-resolved analysis of individual bacteria in growing colonies shows that after a transient pH decrease, long-term pH evolution is highly cell-dependent. The heterogeneity at single cell level shows the existence of subpopulations that might be more resistant and contribute to population survival. Our approach contributes to an understanding of pH_i regulation in individual bacteria and may help scrutinizing effects of existing and novel food preservation strategies.

1. Introduction

Microbes have evolved to maintain a narrow range of optimal intracellular pH (pH_i) values. For instance, during optimal growth conditions *Bacillus subtilis* maintains its cytoplasmic pH at neutral or slightly higher values, the exact range depending somewhat on the measurement tool used (compare ref. 1 with our data). The pH_i affects many biological processes such as enzyme activity, reaction rates, protein stability, and the structure of different molecules such as nucleic acids. Thus, pH_i of bacteria is very important to ensure optimal growth, and conversely, perturbing the physiological pHi is a strategy that is often exploited by the food industry for preservation purposes. Weak acids such as sorbic, acetic, lactic and benzoic acids are naturally occurring preservatives that are commercially used in the food industry. These molecules are long known to inhibit the outgrowth of both bacterial and fungal cells (2), thereby allowing for the extension of the shelf-life of food products. Sorbic acid and its salts inhibit the growth of various bacteria including sporeformers, at various stages of their life cycle including spore germination, outgrowth, and vegetative cell division (3). The widely accepted theory of weak acid preservative action suggests inhibition of growth through lowering the pH_i. According to the theory, undissociated acid molecules pass depending on their lipophilicity more or less readily through the plasma membrane by diffusion. In the cytoplasm (pH> 7.5) the acid molecules dissociate into charged anions and protons. These cannot pass across the lipid membrane and hence accumulate in the cytoplasm, lowering the pH_i of the cell. The acidification of the cytoplasm, in turn, inhibits metabolism. A recent study by van Beilen et al. (4) shows that sorbic acid has an ability to act as a classical uncoupler, transporting protons over the membrane, whereas acetic

71 acid, which is less lipophilic, does so to a much lesser extent. This is corroborated by the
72 fact that sorbic acid has a greater effect on the membrane potential while acetic acid only
73 carries bulk volume protons across the membrane until a steady state is reached. Studies
74 by Holyoak et al. and Bracey et al. (5, 6) showed that in yeast the inhibitory action of
75 weak acid preservatives evokes an energetically expensive stress response. This response
76 in *S. cerevisiae* is based on a membrane localized efflux system that removes both the
77 accumulated anions as well as the excess protons, from inside the cell (7, 8). The attempts
78 to restore homeostasis, however, require significant amounts of ATP hence resulting in a
79 drop of available energy pools for growth and other essential metabolic functions. In
80 summary, weak acids inhibit the growth of microbes in a number of ways including
81 through membrane perturbation, inhibition of essential metabolic reactions (6, 3), and
82 stress on pH_i homeostasis as well as the accumulation of toxic anions (6, 9).
83 Direct measurement of the pH_i may be used as a proxy for cellular metabolism and
84 thereby provide rapid insight in survival strategies at the single-cell level. The pH_i of the
85 cells can be measured by various methods such as ^{31}P NMR, fluorescent dyes (most
86 noticeably 5 (and 6-) carboxyfluorescein diacetatesuccinimidyl ester) and the distribution
87 of radio-labeled membrane-permeable weak-acids (10-14). The advantage of these
88 methods is that they do not require genetic modification. In the case of fluorescent dyes,
89 single cell measurements are possible (15). The disadvantage of using weak organic acid
90 dyes is that they may themselves alter the pH_i. The disadvantage of the ^{31}P NMR and
91 radio-labeled compounds are that they require extensive cell handling and high cell
92 density, which also disturbs the cell's physiology. Fluorescent proteins make an
93 attractive, non-invasive alternative for measuring the pH_i of the bacterial cell though

obviously here genetic modification is a prerequisite. pHluorin, a ratiometric, pH-sensitive GFP variant (16), allows direct, fast, and localized pH_i measurements. It has been successfully used in *S. cerevisiae* (17, 18) and more recently in *B. subtilis* (19-21), to probe cellular responses to various growth conditions, glucose pulses, respiratory chain inhibitors, and a few other treatments. A specific advantage of a fluorescence-microscopy based method is that it can provide information with (sub)cellular resolution (22,23). This allows for the capturing of inter-individual phenotypic heterogeneity that arises from factors such as differential growth kinetics and stochastic effects at the level of gene expression and protein activity. Taking advantage of this added value, we analyzed the effect of sorbic and acetic acid on the perturbation of the pH_i of *Bacillus subtilis* vegetative cells using an improved IpHluorin reporter.

2. Materials and Methods

2.1 Growth conditions

To monitor the pH_i of exponentially growing *B. subtilis* cells for a long period of time, the *B. subtilis* PptsG-IpHluorin (*trp*2C; *amyE3'* spcR P*ptsG-IpHluorin amyE5'*) construct was used (20). This construct consists of the IpHluorin gene (16), which was inserted after the first 24 bp of *comGA* adjacent to the promoter PptsG. This promoter drives the expression of the gene encoding the glucose-specific phosphotransferase system II. Thus we were able to obtain expression of IpHluorin in vegetative cells growing on a glucose-containing medium. The *B. subtilis* 168 laboratory wild-type strain PB2 and *B. subtilis* PptsG-IpHluorin were grown exponentially in Luria Broth (LB) at 37°C, under continuous agitation at 200 rpm. The exponentially growing cells were re-inoculated in a minimal defined medium with 80 mM MOPS (3-(N-morpholino) propanesulfonic acid) (26), here buffered to pH 7.4; hereafter referred to as MOPS medium. The MOPS medium contained spectinomycin (50 μg/ml) when appropriate, and cells were grown until exponential phase at 37°C, under continuous agitation at 200 rpm. The optical density at 600_{nm} (OD_{600nm}) was measured in time to check whether the cells were in the exponential phase. Cells in the early exponential growth phase (OD_{600nm} = ~0.2) were used for time-lapse microscopy experiments (see below). In stress experiments, 3 mM sorbic acid (KS) and 25 mM acetic acid (KAc) at pH 6.4 were used to test for their effect on the growth and pH_i of exponentially growing bacteria.

2.2 Phototoxicity measurements

Phototoxicity is a detrimental phenomenon in live-cell imaging, which occurs upon repeated exposure of fluorescently labeled cells to intense light. In order to test for possible phototoxicity, exponentially growing *B. subtilis* PB2 and *B. subtilis* PptsG-IpHluorin cells (grown in MOPS medium under live-imaging conditions, see below) were repetitively exposed to excitation light of two different wavelengths (390 nm and 470 nm) with an exposure time of 100 ms and 30 ms, respectively for a period of 5 h with an interval of 5 min and 10 min. The exposure time was chosen in such a way that the bleaching in each channel has the same rate. The generation time of the cells was calculated with a home-written script for ImageJ (http://imagej.nih.gov/ij/) (25), multichannel-SporeTracker. The total number of cells assessed for *B. subtilis* PB2 cells grown in the absence of fluorescent light was 107 and for *B. subtilis* PptsG-IpHluorin cells cultured in the absence and presence of fluorescent light between 77 and 164. The effect of phototoxicity on the cells was regarded as negligible when the generation times of vegetative cells did not differ significantly (t-test, $p > 0.05$).

2.3 Fluorescence time-lapse microscopy(live-imaging)

In order to ensure the unbiased growth of aerobic bacteria, a closed air-containing chamber that has been described previously (25) was used for time-lapse fluorescence microscopy. In this chamber, cells were sandwiched between the glass coverslip and a thin (160 µm) 1% agarose-medium pad, molded in a Gene Frame®, to ensure their immobilization in the presence of sufficient culture medium and enough oxygen for undisturbed growth. The pad was loaded with 1 µl of exponentially growing vegetative

cells (OD_{600nm} = ~2). Time-lapse series were made by making use of a temperature-controlled boxed incubation system for live imaging set at 37°C.

The specimens were observed with a 100X/1.3 plane apochromatic oil objective mounted on a Zeiss wide field fluorescence microscope (Axiovert-200 Zeiss, Jena, Germany) controlled by Metamorph 6.1 software. For ratiometric imaging, light from a Xenon arc lamp was filtered by a monochromator (Optoscan, Cairn Research Ltd, UK) and tuned to 390 nm or 470 nm, each with a bandwidth of 30 nm. The microscope was equipped with a standard GFP filter cube (Chroma) with 510 nm LP emission filter. Images were acquired with a CoolSnap HQ CCD camera (Roper Scientific). For phase contrast imaging, a red filter (610 nm LP; Schott AG, Germany) was placed in the light path to protect the cells from phototoxicity. For control experiments, the time-lapse series of phase-contrast and fluorescence images were recorded at a sampling frequency of 1 frame per 10 min (see Results section for the final choice of 10 min intervals) for 5 hours and for stress experiments the cells were imaged for 10 hours (also 1 frame per 10 min). Two biological replicates and 15-30 technical replicates (recorded fields of view on one slide) were recorded in parallel per experiment. In every field of view (technical replicate), 2-8 vegetative cells were identified and followed in time. This resulted in the analysis of approximately 30-60 vegetative cells from the start of each imaging experiment per biological replicate.

2.4 pH_i measurements in a microcolony and in single cells within a microcolony

For pH_i measurements, two image analyses tools for ImageJ were used. “Multichannel-SporeTracker”

(https://sils.fnwi.uva.nl/bcb/objectj/examples/sporetracker/SporeTracker.htm), was developed for pH_i measurements at the microcolony level. This program runs in combination with ObjectJ, (https://sils.fnwi.uva.nl/bcb/objectj/), a plugin for ImageJ. ObjectJ supports graphical vector objects that non-destructively mark images on a transparent layer. It provides back-and-forth navigation between results and images. The results table supports statistics, sorting, color-coding, qualifying, and macro access.

Multichannel-SporeTracker allows accurate measurements of the intensity of IpHluorin in the cell, calculates the ratio (E_{390}/E_{470}) of IpHluorin and deduces the pH_i and the generation time of the vegetative cells growing into a micro colony at any desired time frame (Figure 1). The generation time is calculated from the area (Log_2) of the growing cell population. The pH_i measurements are based on the ratio of the fluorescence emission at 510 nm after excitation at 390 nm and 470 nm respectively (E_{390}/E_{470}). To calculate the pH_i, fluorescence images were first aligned with the corresponding phase contrast images. Before measuring the fluorescence intensity of the cells, temporal intensity fluctuations were buffered by subtracting the mode (most frequent) value per frame throughout the time-lapse image stack. Then, the fluorescence intensities of IpHluorin expressing cells were measured in both fluorescence channels within cellular regions of interest and the E_{390}/E_{470} ratio was calculated. By correlating the ratio with a calibration curve (mentioned below), the pH_i of the cell was determined.

For pH_i measurements at the single cell level, a custom-made script for IJ/FIJI ColiMetrics.ijm was used (https://www.uantwerpen.be/cell-group/). The algorithm segments individual bacteria and tracks them through time. It also converts the two-channel fluorescence image (excitation at 390 nm and 470 nm) into a color-coded image

representing the pH_i for every individual cell in a micro colony (i.e. pH maps). pH_i maps are HSV (Hue, Saturation, Value) images, in which the hue represents the ratio of both fluorescence channels, converted into a pH_i value according to a sigmoidal fit of the calibration curve, and the value the average intensity of both channels (expansion of a macro described before. See reference 27). For single cell analysis, individual bacteria were tracked through time up to the point of cell division. Ratio values E_{390}/E_{470} were measured per cell and plotted as a function of time.

2.5 Calibration of pH_i

B. subtilis PptsG-IpHluorin cells were grown to exponential phase in MOPS medium to pH 7.4 containing spectinomycin (50 μg/ml). At an optical density of 0.4 (OD_{600nm}), the cells were centrifuged (1073 g; 10 min) and resuspended in phosphate-citrate buffers (0.1 M citrate and 0.2 M K_2HPO_4) with pH values ranging from 5.5 to 8.5 as described previously by us (20). The cells were then permeabilized with the potassium ionophore valinomycin (1 μM) and the protonophore nigericin (1 μM) (13). This treatment allows for the equilibration of the pH_i with the externally set pH. Subsequently, cells in the phosphate-citrate buffer of different pH (5.5 to 8.5) were transferred to agarose pads with the ionophores at 1μM and of the corresponding buffered pH values in closed air-containing chambers (20). For each pH, fluorescence images of ~200 cells were analyzed with Multichannel-SporeTracker to construct a calibration curve (Figure 2). This curve represents the relationship between the ratio of the 510 nm emission intensities of IpHluorin upon excitation at respectively 390 nm and 470 nm (E_{390}/E_{470}) and the pH_i.

The data was fitted to a slightly modified Henderson-Hasselbalch equation. It describes the relation between the ratio of the intensity of wavelengths ($R = E_{390}/E_{470}$) and pH_i. Here, $R = ((10^{(pH_i - pK_a)})/((10^{(pH_i - pK_a)}+1)))*b+a$. pK_a = the negative 10 logarithm of the dissociation constant, b and a are parameters without physiological meaning but they are used to enable a quantitative fit of the R values. The fitting procedure was conducted as follows: In total 876 observations were available; 23 observations almost equally distributed across the different pH values were either negative of far beyond the set (3 standard deviations) to which they belonged. After elimination of these outliers the average of each local clusters was taken. In total 62 average values were obtained. To test the robustness of the model 20 average values were selected randomly and left out. The 42 remaining values were fitted according to our modified Henderson-Hasselbalch equation. The estimates of the parameters including confidence intervals are shown in Table 1 and Table 2. For nonlinear regression models the correlation coefficients between the parameters can be considered as acceptably low (28). The average residual sum of squares (RSS) was calculated for each pH value that was studied. No significant correlation was found between averages RSS and pH. The average sum of squares was 0.009688.

3. Results

3.1 Long-term ratiometric imaging of IpHluorin expressing cells is not phototoxic

A typical fluorochrome can only withstand a limited number of excitation cycles. Excessive illumination eventually leads to irreversible loss of fluorescence (photobleaching) and the production of free radicals that can damage cellular components

241 compromising cell viability (phototoxicity). The combined effect, i.e. photodamage,
242 restricts long-term fluorescence live-cell imaging. Photodamage can be mitigated by the
243 parsimonious use of illumination light but cannot be eliminated completely (29). To
244 assess whether our imaging conditions allowed for monitoring bacterial cells without
245 excessive photodamage, we compared the generation time with and without fluorescence
246 illumination. In addition, we assessed the effect on cell growth of IpHluorin expression.
247 The generation time of wild-type *B. subtilis* PB2 cells grown in the absence of excitation
248 light (93±13 min) was similar to the generation time of the IpHluorin-expressing cells
249 grown in the absence of excitation light (92±17 min) (Figure 3). Therefore, we concluded
250 that IpHluorin expression is not harmful to the cells under the tested conditions. Next,
251 cells were exposed to sequential pulses of light of two different wavelengths (390 nm and
252 470 nm, for 100 and 30 ms, respectively) with 5 min or 10 min intervals between
253 fluorescence measurements. Figure 3 also shows the effect of repeated exposure of cells
254 to 390 nm and 470 nm excitation on the generation time of the *B. subtilis* PptsG-
255 IpHluorin expressing cells. Both conditions, i.e. 5 min and 10 min intervals, resulted in a
256 slight increase in generation time (116±3 min resp. 114±21 min) without causing cell
257 death (no cell lysis was observed whilst analyzing either of the incubations
258 microscopically). We conclude that our settings are suitable for up to 5 hours of pH_i live-
259 imaging and went for the longer 10 min interval in further experiments.
260
261 ***3.2 Sorbic and acetic acid impact on pH_i and growth of B. subtilis cells***
262 Sorbic and acetic acid have detrimental effects on bacterial cells. Both have a similar pKa
263 of 4.76, but sorbic acid is lipophilic whereas acetic acid is hydrophilic in nature. Here the
264 effect of exposure at pH 6.4 to 3 mM potassium sorbate and 25 mM potassium acetate

265 was studied in vegetative *B. subtilis* cells at single cell level. Figure 4 shows the effect of
266 sorbic and acetic acids on the pH_i and generation time of *B. subtilis* PptsG-IpHluorin
267 vegetative cells growing in microcolonies. In sorbic acid-stressed cells, the average
268 internal pH of the microcolonies decreased from 7.2 to 6.8 (Figure 4A, Table 3) and the
269 generation time increased significantly (Figure 4A, Table 3). In 25 mM potassium
270 acetate-stressed cells, a similar trend in internal pH and increase in generation time was
271 observed (Figure 4A, Table 3). Figure 4B gives the correlation graph between the
272 average internal pH of the microcolonies and generation time for control cells as well as
273 cells stressed with the two acids. PptsG-IpHluorin expressing cells are typically lowered
274 50% in their growth-rate by the addition of 3mM potassium sorbate or 25 mM potassium
275 acetate to liquid cultures whilst monitoring at population level pH_i (4). Here, growth-rate
276 inhibition by these concentration of both weak organic acids is more and the observed
277 standard deviation for the population is high. This might reflect some light sensitization
278 by the weak organic acid stresses. However, we have also shown previously that in the
279 MOPS buffered defined medium used here, there is a ~30% increase in generation time
280 of wild-type *B. subtilis* cells compared to liquid culture conditions (25). Hence, though
281 we cannot exclude that under our live-imaging conditions weak acid stress response may
282 sensitize the PptsG-IpHluorin expressing cells to light, it will not be the major response
283 seen.
284 In conclusion, acid stressed cells and control populations displayed both for pH_i and
285 growth-rate significant differences ($p< 0,001$). Figure 4C shows selected time-points
286 from movies (see Videos S1, S2, S3 and Table S1) of *B. subtilis* PptsG-IpHluorin
287 vegetative cells in the presence and absence of 3 mM potassium sorbate and 25 mM

potassium acetate, color coded by their pH_i. Noticeably, as was observed previously by van Beilen et al. (figure 1 b in ref. 4), pH_i of control cells started in some at values above 8, indicating a somewhat stalled metabolic activity at the onset of imaging. In this regard we noted a clear batch variation between the two biological repeats shown. Growth-rate and average colony pH_i calculations with Multichannel-SporeTracker were always performed from the time-point where clearly detectable surface increase, i.e. growth, had resumed. pH_i was then generally ~7.5, values seen previously by van Beilen et al. in liquid populations (4, 20).

3.3 Lineage tracing of individual cells in microcolonies reveals pHi heterogeneity.

As noted in Methods, single *B. subtilis* cells grow and divide to form micro colonies. We observed that within a developing microcolony the E_{390}/E_{470} fluorescence ratio of individual *B. subtilis* cells differs. This shows that there is heterogeneity in pH between individual *B. subtilis* cells in a microcolony at a given time-point of culture. Figure 5 shows for control conditions a typical example of tracking individual cells, growing from a single cell up to a microcolony. It became clear that under those conditions, after a transient drop in pH_i presumably due to the increased levels of acetate made by the growing bacteria themselves (see e.g. ref. 4), individual bacteria are likely able to mount to varying extent a response that allows them to finally again raise their internal pH albeit to varying degrees. Such variation in pH_i is also observed for the intentionally, at time zero, weak organic acid stressed cells. This is in particular true for those exposed to sorbic acid (Figure 4A, B). Under 3mM potassium sorbate stress conditions strikingly, microcolonies emerged with pHi values well within the range of those from control cells

311 as well as well below. While pH_i is clearly a major determinant for growth-rate it is
312 definitely not the only one, certainly not under sorbic acid stress.
313
314 **4. Discussion**
315 Here, we deployed a derivative of green fluorescent protein (GFP), IpHluorin, to probe at
316 a single cell level the pH_i of *B. subtilis* cells. The use of this genetically encoded reporter
317 holds various advantages such as the inherent labeling, strong signal-to-noise ratio, and
318 concentration-independence. A potential disadvantage is its requirement for molecular
319 oxygen, precluding its use in anaerobic species such as *Clostridium* spp.
320 Using stably expressing IpHluorin *B. subtilis*, we have established a robust microscopy-
321 based assay for simultaneously measuring pH_i and generation time. We have first tuned
322 the imaging conditions so as to minimize phototoxicity. Subsequently we have
323 established a calibration curve showing strong correlation of the fluorescence ratio with
324 the externally adjusted pH ranging from 5.5 to 8.5. Once optimized, we have
325 benchmarked our assay using two well-known weak acid preservatives, namely sorbic
326 and acetic acid. Also, to analyze the microscopy images we developed a semi-automated
327 image analysis tool based on the previously published Spore-Tracker (25), called
328 "Multichannel-SporeTracker". This tool calculates the internal pH and the generation
329 time of exponentially growing *B. subtilis* PptsG-IpHluorin vegetative cells. It allows us to
330 monitor individual cells and subpopulations and deconvolute the population level
331 information at single cell level.
332 The analysis of the effect of sorbic acid and acetic acid on vegetative cells showed that at
333 low concentration of sorbic acid, the generation time increases with decreasing pH_i.

Similar results were obtained from the analysis of acetic acid treated cells, albeit at higher acid concentrations and a wider distribution of generation times is seen. Thus, at the selected concentrations both acids reduce the pH_i and the growth-rate to a similar extent. This result corroborates the notion that sorbic acid is the more effective preservative of the two. Van Beilen et al. showed that sorbic acid is unable to recover pH_i during acid stress. These observations reflect the notion that sorbate acts as a classical uncoupler, which shuttles protons over the membrane whereas, acetate is believed to do this to a much lesser extent (4). The data of van Beilen et al. show that sorbic acid has an effect on the membrane potential while acetic acid carries only bulk volume protons across the membrane until a steady state is reached leaving $\Delta\psi$ relatively unaffected. In line with this, Orij et al. and van Beilen et al. (4, 17) have shown at the population level that the growth-rate and pH_i can be correlated (4). We now also demonstrate a similar correlation at the single cell level, demonstrating that pH_i can be assessed as a good indicator of individual 'bacterial health'. From this knowledge of pH_i one could infer at the individual cell level the activity of metabolic pathways key to cellular energy conversion. Such data may be used by food microbiologists to feed contemporary models that aim at quantitatively predicting microbial food stability. The study suggests that heterogeneity at the individual cell level is prominent with important implications for weak organic acid based food preservation strategies. We can now, through lineage tracing, also start to verify mechanistically whether under long term weak organic acid stress conditions, subpopulations of *Bacillus* cells arise that might be more able to restore their pH_i hence explaining their better survival in foods and outgrowth potential to new (micro-)colonies

356 that can spoil foods. It may also be applied to the analysis of other potential food spoilage
357 organisms, such as e.g. *Zygosaccharomyces bailii* (30).

358 In conclusion, our microscopy-based single-cell analysis technique effectively
359 allows for gauging pH_i and relating it to generation time. In doing so, the method can
360 further mechanistic insight in the principles of existing and novel food preservation
361 strategies. The analysis can be extended to the ratiometric assessment of the dynamics of
362 the pH_i of spores during germination and outgrowth. It will allow one to point out the
363 phase where weak acids have a maximum effect and also could provide key information
364 about the timing of weak organic acid action on individual germinating and outgrowing
365 spores. This information can be coupled to risk management of the unwanted growth of
366 bacteria in food and hence help food industry to combat food spoilage. An attractive
367 platform for implementing such an assay would be a microfluidics-based lab-on-chip
368 (31). Such a platform allows for rapid measurement of pH_i values under dynamically
369 changing conditions (change of media types or supplements) coupled to monitoring of the
370 dynamics of spore germination and outgrowth. This type of experiments should provide
371 ways to deconvolute the population data with respect to effects of different sequences of
372 stresses on the germination and (out-)growth efficiency of *B. subtilis* spores.

373

374 **Aknowledgements**

375 Huub Hoefsloot and Chris de Koster are thanked for expert advice on statistics analyses.
376 Rachna Pandey was supported by the Erasmus Mundus program (EMECW 15) and the
377 University of Amsterdam. Alex Ter Beek was supported by a grant from the Dutch
378 Foundation of Applied Sciences (STW 10431).

References

1. **Shioi JI, Matsuura S, Imae Y.** 1980. Quantitative measurements of proton motive force and motility in *Bacillus subtilis*. J. Bacteriol. **144**: 891-897.
2. **Krebs HA, Wiggins D, Stubbs M, Sols A, Bedoya F.** 1983. Studies on the mechanism of the antifungal action of benzoate. Biochem J. **214**: 657-663.
3. **Mols, M, Abee, T.** 2011. *Bacillus cereus* responses to acid stress. Environ. Microbiol. **13**: 2835-2841.
4. **van Beilen JWA, Teixeira de Mattos MJ, Hellingwerf KJ, Brul S.** 2014. Sorbic acid and acetic acid have distinct effects on the electrophysiology and metabolism of *Bacillus subtilis*. Appl. Environ. Microbiol. **80**: 5918-5926.
5. **Holyoak CD, Stratford M, McMullin Z, Cole MB, Crimmins K, Brown AJP, Coote PJ.** 1996. Activity of the plasma membrane H^+-ATPase and optimal glucolyticux are required for rapid adaptation and growth of *Saccharomyces cerevisiae* in the presence of the weak-acid preservative sorbic acid. Appl. Environ. Microbiol. **62**: 3158-3164.
6. **Bracey D, Holyoak CD, Nebevon Caron G, Coote PJ.** 1998. Determination of the intracellular pH (pH_i) of growing cells of *Saccaromyces cerevisiae*: the effect of reduced-expression of the membrane H^+-ATPase. J. of Microbiol. Methods **31**: 113-125.
7. **Henriques M, Quintas C, Loureiro-Dias MC.** 1997. Extrusion of benzoic acid in *Saccharomyces cerevisiae* by an energy-dependent mechanism. Microbiology.**143**: 1877-1883.

8. **Piper P, Mahe Y, Thompson S, Pandjaitan R, Holyoak C, Egner R, Mühlbauer M, Coote P, Kuchler K.** 1998. The Pdr12 ABC transporter is required for the development of weak organic acid resistance in yeast. The EMBO J. **17:** 4257- 4265.
9. **Eklund T**. 1985. Inhibition of microbial growth at different pH levels by benzoic and propionic acids and esters of p-hydroxybenzoic acid. Int. J. Food Microbiol. **2**: 159- 167.
10. **Ugurbil K, Rottenberg H, Glynn P, Shulman RG.** 1978. 31P nuclear magnetic resonance studies of bioenergetics and glycolysis in anaerobic *Escherichia coli* cells. Proc. Natl. Acad. of Sci. (USA) **75**: 2244-2248
11. **Bulthuis BA, Koningstein GM, Stouthamer AH, van Verseveld HW**.1993. The relation of proton motive force adenylate energy charge and phosphorylation potential to the specific growth-rate and efficiency of energy transduction in *Bacillus licheniformis* under growth condition. Antonie van Leeuwenhoek **63**: 1-16.
12. **Magill NG, Cowan AE, Koppel DE, Setlow P.** 1994. The internal pH of the forespore compartment of *Bacillus megaterium* decreases by about 1pH unit during sporulation. J. Bacteriol. **176**: 2252-2258
13. **Breeuwer P, Drocourt J, Rombouts FM, Abee T.** 1996. A novel method for continuous determination of the intracellular pH in bacteria with the internally conjugated fluorescent probe 5 (and 6)-carboxyfluorescein succinimidyl ester. Appl. Environ. Microbiol. **62**: 178-183.

14. **Leuschner RG, Lillford PJ.** 2000. Effect on hydration on molecular mobility in phase-bright *Bacillus subtilis* spore. Microbiology (UK). **146**: 49-55.

15. **Slonczewski JL, Ujisawa M, Krulwich TA.** 2009. Cytoplasmic pH measurement and homeostasis in bacteria and archaea. Adv. in Microb. Physiol. **317**: 1-79.

16. **Miesenbök G, De Angelis DA, Rothman JE.** 1998. Visualizing secretion and synaptic transmission with pH-sensitive green fluorescent proteins. Nature **394**: 192- 195.

17. **Orij R, Brul S, Smit GJ.** 2011. Intracellular pH is a tightly controlled signal in yeast. Biochim. Biophys. Acta **1810**: 933-944.

18. **Ullah A, Orij R, Brul S, Smit GJ.** 2012. Quantitative analysis of the mode of growth inhibition by weak organic acid in yeast. Appl. Environ. Microbiol. **78**: 8377-8387.

19. **Martinez KA^{2nd}, Kitko RD, Mershon JP, Adcox HE, Malek KA, Berkmen MB, Slonczewski JL.** 2012. Cytoplasmic pH response to acid stress in individual cells of *Escherichia coli* and *Bacillus subtilis* observed by fluorescence ratio imaging microscopy. Appl. Environ. Microbiol. **78**: 3706-3714.

20. **van Beilen JWA, Brul S.** 2013. Compartment-specific pH monitoring in *Bacillus subtilis* using fluorescent sensor proteins; a tool to analyse the antibacterial effect of weak organic acids. Frontiers in Microbiol. **4**: 157

21. **Ter Beek A, Janneke GE, Wijman Zakrzewska A, Orij R, Smits GJ, Brul S.** 2015. Comparative physiological and transcriptional analysis of weak organic acid stress in *Bacillus subtilis*. Food Microbiol. **45**: 71-82.

22. **Martinez-Munoz GA, Kane P.** 2008. Vacuolar and plasma membrane proton pumps collaborate to achieve cytosolic pH homeostasis in yeast. J. Biol. Chem. **283**: 20309-20319.

23. **Orij R, Postmus J, Ter Beek A, Brul S, Smits GJ.** 2009. In vivo measurement of cytosolic and mitochondrial pH using a pH-sensitive GFP derivative in *Saccharomyces cerevisiae* reveals a relation between intracellular pH and growth. Microbiology (UK). **155**: 268-278.

24. **Kitko RD, Cleeton RL, Armentrout EI, Lee GE, Noguchi K, Berkmen, Melanie B, Jones BD, Slonczewski JL.** 2009. Cytoplasmic acidification and the benzoate transcriptome in *Bacillus subtilis*. PLoS One **4**:e8255.

25. **Pandey R, Ter Beek A, Vischer NOE, Smelt J, Brul S, Manders EMM**. 2013. Live cell imaging of germination and outgrowth of individual *Bacillus subtilis* spores; the effect of heat stress quantitatively analyzed with SporeTracker. PLoS ONE **8**:e58972.

26. **Kort R, O'Brien AC, van Stokkum IHM, Oomes SJCM, Crielaard W, Hellingwerf KJ and Brul S**. 2005**.** Assessment of heat resistance of bacterial spores from food product isolates by fluorescence monitoring of dipicolinic acid release. Appl. Envron. Microbiol. **71**, 3556-3564.

27. **Back P, De Vos WH, Depuydt GG, Matthijssens F, Vanfleteren JR, Braeckman BP.** 2012. Exploring real-time in vivo redox biology of developing and aging *Caenorhabditis elegans*. Free Radical Biology and Medicine **52**: 850–859.

27. **Motulsky, H. and Christopoulos, A.** eds. 2004. Fitting models to biological data

Using linear and nonlinear regression. A practical guide to curve fitting. Oxford University Press.

28. **Hoebe RA, Van Oven CH, Gadella TW Jr, Dhonukshe PB, Van Noorden CJ, Manders EM.** 2007. Controlled light-exposure microscopy reduces photobleaching and phototoxicity in fluorescence live-cell imaging**.** Nat. Biotechnol. **25**: 249-253.

29. **Dang TD, De Maseneire SL, Zhang BY, De Vos WH, Rajkovic A, Vermeulen A, van impe JF, DeVlieghere F.** 2012. Monitoring the intracellular pH of *Zygosaccharomyces bailii* by green fluorescent protein. Int. J. Food Microbiol. **156:** 290–295.

30. **Dutse SW, Yusof NA.** 2011. Microfluidics-Based Lab-on-Chip Systems in DNA-Based Biosensing: An Overview. Sensors, **11:** 5754-5768.

Figure Legends

Figure 1: Multichannel-SporeTracker output for pH_i measurements in growing *B. subtilis* cells. Shown here are collective plots of 4 individual cells measured every 5 min for 5 hours. Bottom to top: Log_2 (surface area occupied by cells); fluorescence intensities measured at 510 nm when excited at 390 nm (Fluor A) and 470 nm (Fluor B), respectively; the ratio of the excitation wavelength (390 nm and 470 nm) of fluorescence intensities (2^{nd} panel from the top) and pH_i (top panel). Note that here 4 cells are shown

490 from the batch that starts at $pH_i > 8$; in cells from other batches pH_i was lower (~7.5) at
491 the onset of imaging (see text and figure 5 lineage tracking for comparison).
492
493 **Figure 2:** Calibration curve of *B. subtilis* PptsG-IpHluorin, which describes the relation
494 between the ratio of the emission intensity at 510 nm after excitation at 390 nm and 470
495 nm respectively (E_{390}/E_{470}) and pH_i. The *B. subtilis* PptsG-IpHluorin cells were
496 permeabilized using 1 μM nigericin and 1 μM valinomycin and immobilized on agarose
497 pads containing both compounds and of the set pH values ranging from 5.5 to 8.5. The
498 cell fluorescence emission intensities were measured and the ratio (E_{390}/E_{470}) was plotted
499 against pH_i. At least 200 cells were measured per data point. Error bars indicate the
500 standard deviation. The figure gives a comparison between the observations that were
501 fitted (observed 1 Δ), the observations that were not used for fitting (♦) and the actual fit
502 according to the Henderson-Hasselbalch equation based on observed 1 (---).
503
504 **Figure 3:** The effect of fluorescent light (excitation at 390 nm and 470 nm and emission
505 at 510 nm) on *B. subtilis* PptsG-IpHluorin. Movies of *B. subtilis* PB2 cells grown in the
506 absence of fluorescent light and *B. subtilis* PptsG-IpHluorin cells in the absence and
507 presence of fluorescent excitation light (390 nm and 470 nm) with a time interval of either
508 5 min or 10 min were made during 5h. Generation time analyzed by Multichannel-
509 SporeTracker. The total number of cells assessed for *B. subtilis* PB2 cells grown in
510 absence of fluorescent light was 107, for *B. subtilis* PptsG-IpHluorin cells in absence of
511 fluorescent light 164 and for regularly illuminated PptsG-IpHluorin cells 77 (for the

512 specimens inspected every 10 minutes), and 92 (for those illuminated every 5 minutes).
513 No cell lysis was observed whilst analyzing either of the incubations.
514
515 **Figure 4:** Analysis of *B. subtilis* PptsG-IpHluorin vegetative cells growing into
516 microcolonies with Multichannel-SporeTracker shows that pH_i and generation time of
517 sorbic acid and acetic acid-treated cells are affected. (**A**) pH_i frequency distributions of
518 microcolonies of sorbic and acetic acid-stressed (black) as well as control (gray) *B.*
519 *subtilis* PptsG-IpHluorin cells were calculated per 0,05 pH unit bin from data obtained in
520 two biological repeats. Depicted are the frequency distributions as well as the generation
521 time of *B. subtilis* PptsG-IpHluorin cell microcolonies exposed to respectively 3 mM
522 potassium sorbate or 25 mM potassium acetate at pH 6.4. (**B**) Growth-rate vs. pH_i of *B.*
523 *subtilis* PptsG-IpHluorin cells growing in microcolonies for unstressed cells and cells
524 stressed with sorbic acid and acetic acid. Between the acid stressed cells and the control
525 populations both the mean and the variance of pH_i and growth-rate are significantly
526 different (t-test $p< 0,01$). (**C**) Still images at set time-points of (I) phase contrast and (II)
527 fluorescence data showing growth and division of *B. subtilis* PptsG-IpHluorin vegetative
528 control cells (Top row) and cells grown in the presence of 3 mM potassium sorbate
529 (Middle row) and 25 mM potassium acetate (Bottom row) at an external pH of 6.4. The
530 acids were included in the agarose slides from the onset of the experiment. Imaging was
531 done as described in Materials and Methods with a 10 min illumination interval.
532
533 **Figure 5:** Time-resolved ratiometric image showing growth and division of single *B.*
534 *subtilis* PptsG-IpHluorin vegetative cell in the absence of stress at an external pH of 6.4.

(**a**) Montage of the ratio image in which the color represents the pH; (**b**) The pH profiles of individual color-coded cells superimposed on the standard deviation of the mean signal of the entire microcolony in grey; (**c**) Lineage tracking and ratio changes in grey scale.

Tables

Table 1 Parameter estimates of the slightly modified Henderson-Hasselbalch model (see Materials and Methods section 2.6) describing the relation between pH_i and the ratio of the IpHluorin fluorescence emission intensity upon excitation at wavelengths 390/470 nm ($R = E_{390}/E_{470}$).

Parameter	Estimate	Std. Error	95% Confidence Interval	
			Lower Bound	Upper Bound
pK_a	7.112	0.055	7.001	7.223
b	1.625	0.048	1.528	1.722
a	0.703	0.040	0.621	0.785

Table 2 Correlations of parameter estimates reported in table 1.

	pK_a	b	a
pK_a	1.000	-0.047	0.625
b	-0.047	1.000	-0.681
a	0.625	-0.681	1.000

The average RSS= 0.00968

Table 3: Mean values and standard deviation of internal pH and generation time of individual *B. subtilis* PptsG-IpHluorin vegetative cells in the presence and absence of sorbic acid and acetic acid[a].

Mean(min)±SD[b]	**Treatment**		
	None	**Potassium sorbate**	**Potassium Acetate**

pH_i	7.20±0.24 (n=151)	6.78±0.14 (n=205)[#*]	6.76±0.11 (n=131)[#*]
Generation time (min)	114±21 (n=164)	304.63±109.70 (n=109)[#*]	286.13±80.78 (n=122)[#*]

[a] *B. subtilis* PptsG-IpHluorin vegetative cells were grown in MOPS medium stressed with or without 3 mM potassium sorbate and 25 mM potassium acetate.

[b] Standard deviation.

* Indicates the variance of the distributions between the stress and control experiment are significantly different ($p<0.01$).

# Indicates the mean of the distributions between the stress and control experiment are significantly different (t-test, $p<0.01$).

The amount of cells analyzed for pH_i and generation time determination are gathered from two (control, sorbic acid, acetic acid) microscopy experiments and given in brackets.

Supplementary Data

Video S1. Growth of *B. subtilis* PptsG-IpHluorin vegetative cells in defined minimal (MOPS-buffered) medium (pH 6.4). The video shows three movies of respectively the phase contrast image as well as the fluorescent emission images upon excitation at 390 nm and 470 nm.

Video S2. Growth of *B. subtilis* PptsG-IpHluorin vegetative cells in defined minimal (MOPS-buffered) medium (pH 6.4) containing 3 mM potassium sorbate. The video

shows three movies of respectively the phase contrast image as well as the fluorescent emission images upon excitation at 390 nm and 470 nm.

Video S3. Growth of *B. subtilis* PptsG-IpHluorin vegetative cells in defined minimal (MOPS-buffered) medium (pH 6.4) containing 25 mM potassium acetate. The video shows three movies of respectively the phase contrast image as well as the fluorescent emission images upon excitation at 390 nm and 470 nm.

Table S1. Results obtained from Multichannel-SporeTracker of growth of *B. subtilis* PptsG-IpHluorin vegetative cells at single cell level. Exponentially growing *B. subtilis* PptsG-IpHluorin vegetative cells were inoculated in defined minimal (MOPS-buffered) medium (pH 6.4) supplemented with (**A**) nothing (control), (**B**) 3 mM potassium sorbate and (**C**) 25 mM potassium acetate. Note that as was observed previously by van Beilen et al. (figure 1 b in ref. 4) pH_i may start at values above 8 likely indicating a stalled metabolic activity of the (control) cells at the start of imaging. Growth-rate and average colony pH_i calculations with Multichannel-SporeTracker were always performed from the time-point where discernible surface increase ,i.e. growth, had resumed. pH_i values at the start of our observations differed between both batches of *B. subtilis* cells shown.

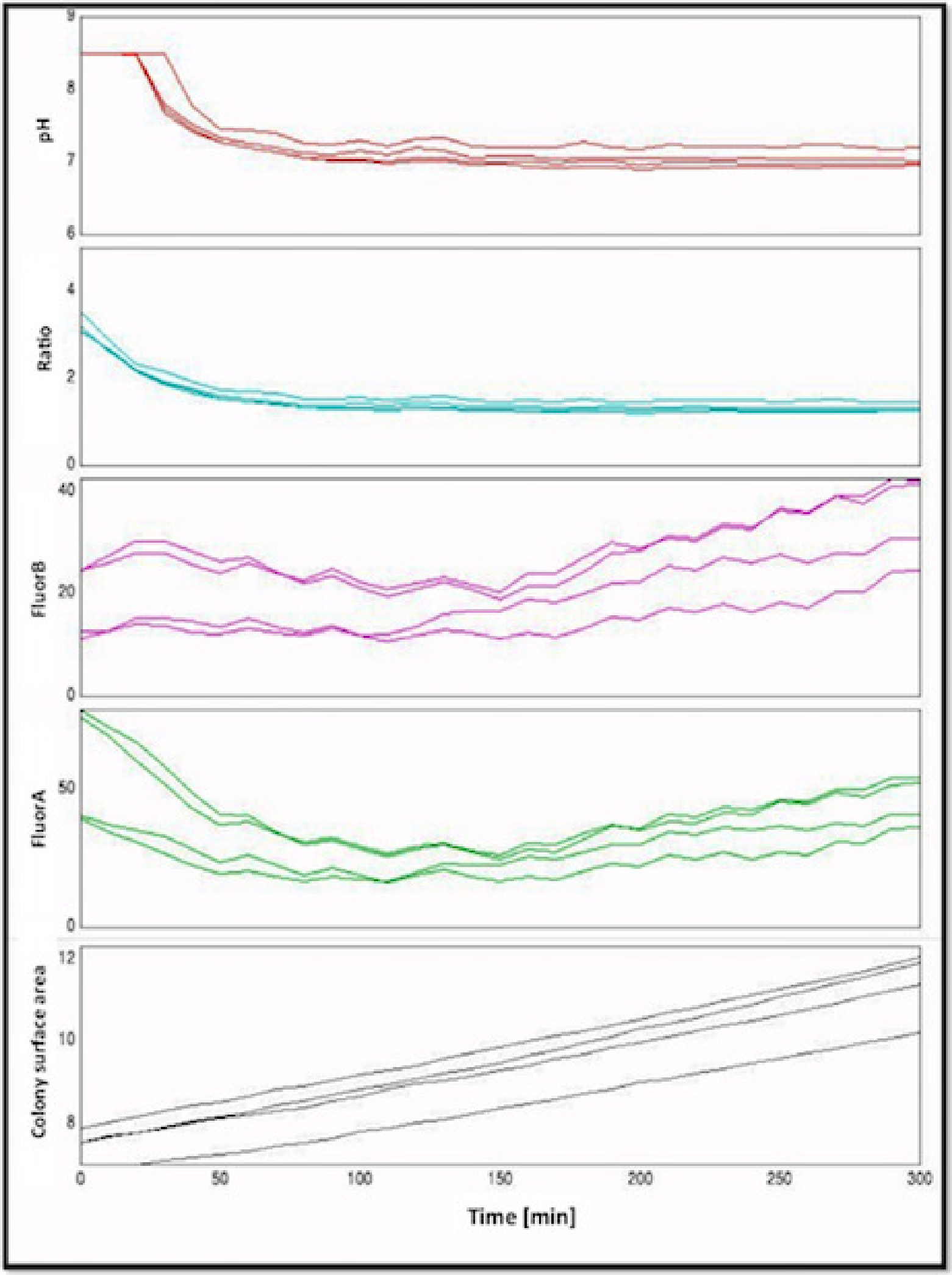
pH
9
8
7
6
Ratio
4
2
0
FluorB
40
20
0
FluorA
50
0
Colony surface area
12
10
8
0
50
100
150
200
250
300
Time [min]

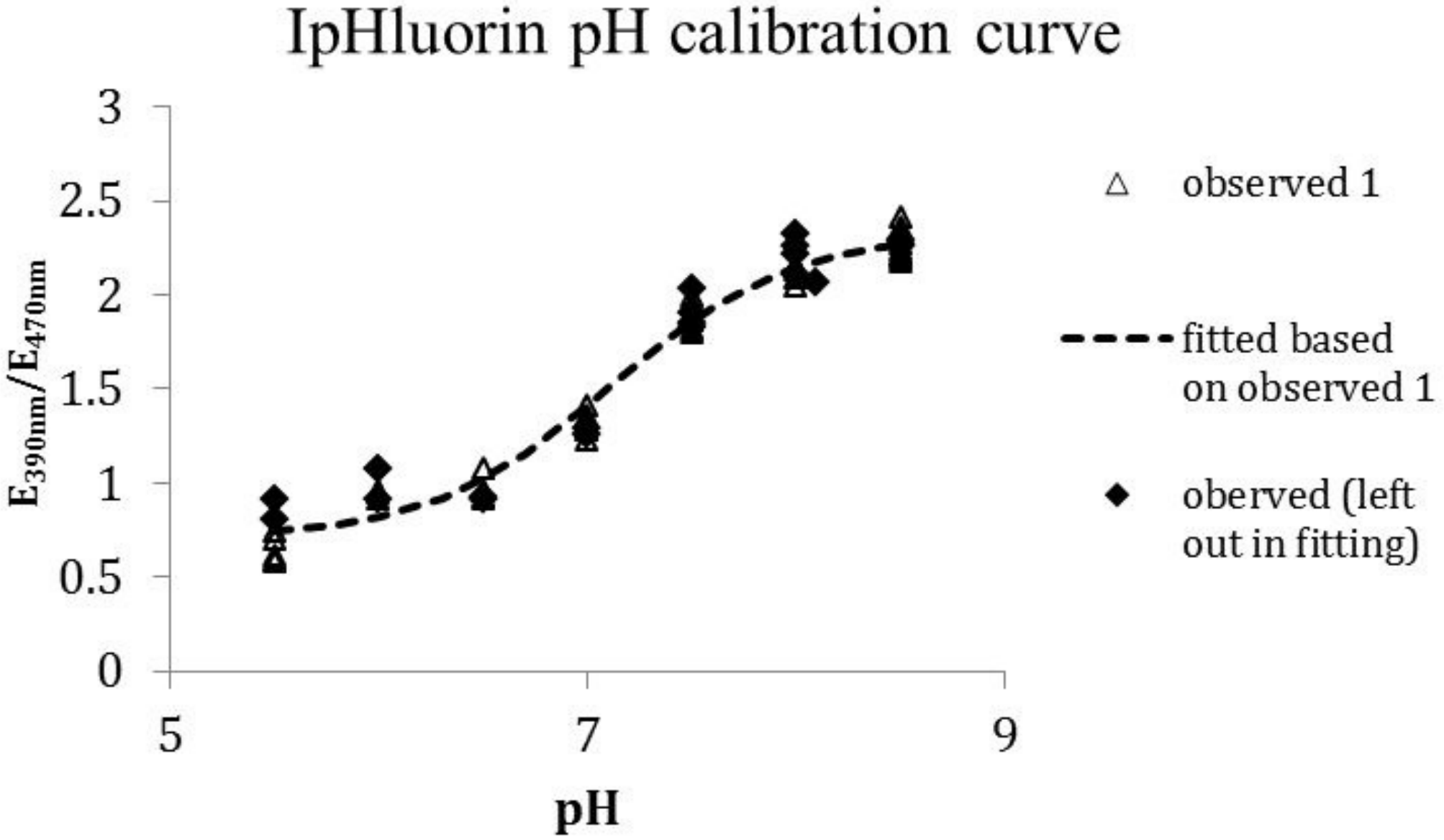
IpHluorin pH calibration curve
3
2.5
2
1.5
1
0.5
0
E390nm/E470nm
5
7
9
pH
observed 1
fitted based on observed 1
oberved (left out in fitting)

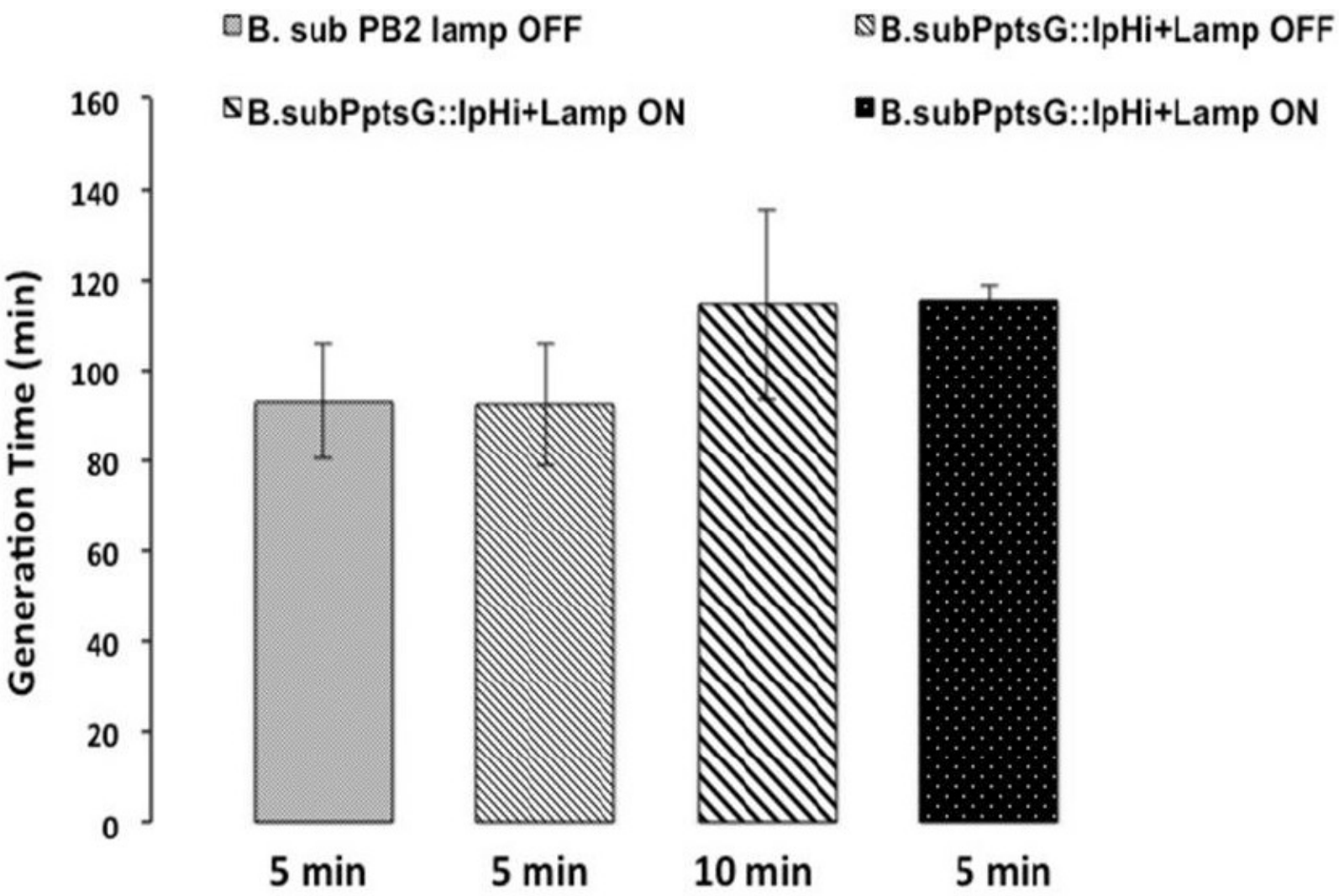
B. sub PB2 lamp OFF
B.subPptsG::IpHi+Lamp OFF
B.subPptsG::IpHi+Lamp ON
B.subPptsG::IpHi+Lamp ON
Generation Time (min)
160
140
120
100
80
60
40
20
0
5 min
5 min
10 min
5 min

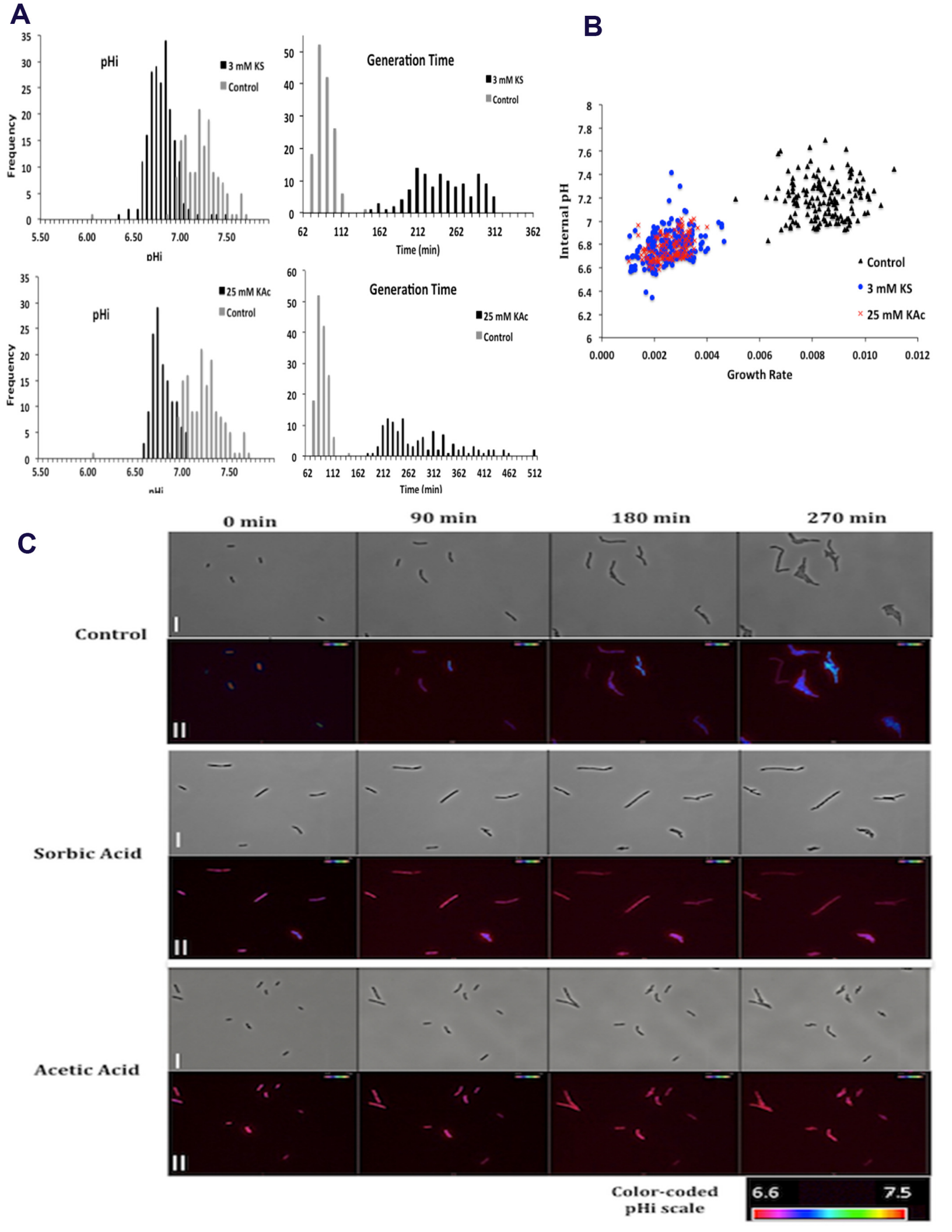
A
pHi
3 mM KS
Control
Frequency
pHi
Generation Time
3 mM KS
Control
Time (min)
pHi
25 mM KAc
Control
Frequency
pHi
Generation Time
25 mM KAc
Control
Time (min)
B
Internal pH
Growth Rate
Control
3 mM KS
25 mM KAc
C
0 min
90 min
180 min
270 min
Control
Sorbic Acid
Acetic Acid
Color-coded
pHi scale
6.6
7.5

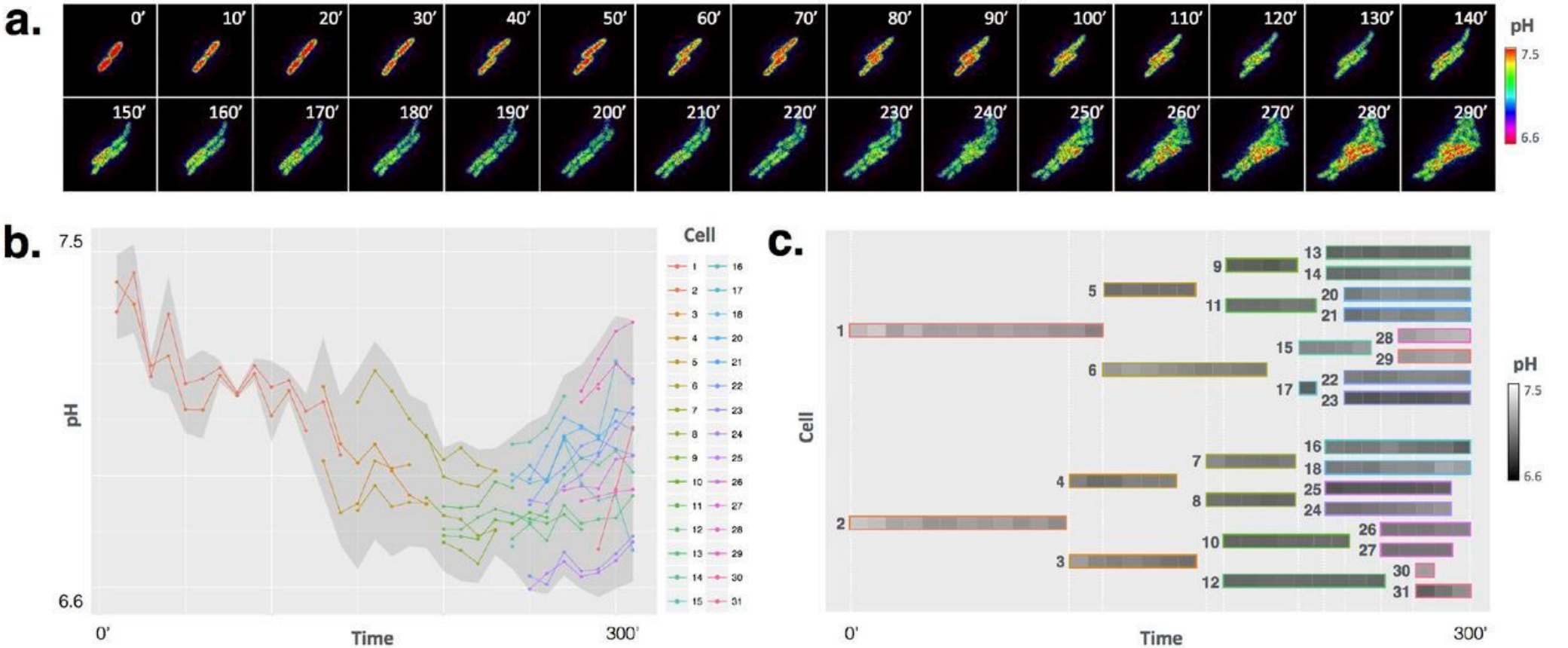
a.
0′
10′
20′
30′
40′
50′
60′
70′
80′
90′
100′
110′
120′
130′
140′
150′
160′
170′
180′
190′
200′
210′
220′
230′
240′
250′
260′
270′
280′
290′
pH
7.5
6.6
b.
7.5
pH
6.6
0′
Time
300′
Cell
c.
Cell
0′
Time
300′
pH
7.5
6.6